Wafer-scale transfer-free patterned graphene transparent electrodes for GaN-based LEDs: a universal technique towards different substrates

npj | 2D materials and applications

Article

Published in partnership with FCT NOVA with the support of E-MRS

https://doi.org/10.1038/s41699-025-00583-z

Wafer-scale transfer-free patterned graphene transparent electrodes for GaN-based LEDs: a universal technique towards different substrates

Penghao Tang[1], Jie Sun[2,3] ✉, Zaifa Du[4], Aoqi Fang[1], Jixin Liu[1], Rongjing Wang[1], Guanzhong Pan[5], Meng Xun[5] & Weiling Guo[1] ✉

With the continuous development of graphene in the field of electronic devices, it is necessary to further develop wafer-scale high-quality graphene preparation technique. A patterning preparation technique for 2-inch wafer-scale transfer-free graphene is reported in this paper, which is innovatively applicable to a variety of substrates. Based on this technique, a 2-inch wafer-scale light-emitting diode (LED) chip with graphene transparent electrodes was fabricated. The results show that the prepared graphene has high quality and uniformity, and plays a good role in improving electrode contact and current spreading. In addition, the LEDs exhibit excellent electrical and optical performance and have a good yield. This wafer-scale graphene preparation technique avoids the damage to graphene caused by the transfer process and the patterning process, which is scalable and suitable for real applications.

Graphene is increasingly used in electronic devices due to its excellent physical and chemical properties, such as GaN-based light-emitting diodes (LEDs), which play an important role in lighting and displays[1–4]. In p-type GaN, the acceptor ions are difficult to ionize, and the mobility of holes is low, which leads to poor conductivity of p-type GaN, making it difficult for GaN-based LEDs to achieve sufficient current spreading and injection[5]. Therefore, transparent electrodes (TEs) with high conductivity and high transmittance have emerged, and the most representative material is indium tin oxide (ITO)[6]. Compared with it, graphene has high transmittance over a wider wavelength band[7] and better performance on flexible substrates[8,9]. In addition, the raw material of graphene is cheaper and environmentally friendly, and it has become one of the most promising transparent electrode materials[10–13].

However, on the road to industrial application, graphene has to face some tests. Metals (e.g., Cu, Ni) play an important catalytic role in the growth of graphene[14,15], which makes most chemical vapor deposition graphene grow on metal surfaces and cannot be directly applied in electronic devices. The transfer process[7,16] is commonly used to transfer graphene to the target substrate, but contamination and damage are inevitably introduced into the graphene during this process. In order to solve this problem, Some more advanced transfer techniques have been proposed[17–19]. More importantly, a variety of transfer-free preparation techniques for graphene have been proposed[20–27], among which the transfer process is avoided and better graphene is obtained. Unfortunately, most of the transfer-free graphene in these techniques is prepared on insulator substrates such as SiO_2, so it is of great significance to explore the transfer-free preparation technique suitable for diverse substrates. In addition to the transfer process, the quality of graphene may also be affected by the patterning process. Since the graphene that is prepared in most cases is an intact film, it needs to be patterned in electronic device applications. If the patterning preparation of graphene can be directly achieved[24,25], it can not only simplify the process, but also reduce the damage to graphene by photolithography and other processes, which is worth looking forward to. In addition, industrial applications mean that wafer-scale preparation is required, which places higher demands on the scale, quality, and uniformity of the prepared graphene. At present, the preparation of graphene with a scale of at least 2-inch wafer is an important research direction[28–34], which will lay the foundation for the industrial application of graphene.

Therefore, in this paper, a wafer-scale patterning preparation technique of transfer-free graphene is proposed, and a 2-inch LED chip with TEs

[1]Key Laboratory of Optoelectronics Technology, Beijing University of Technology, Beijing, China. [2]College of Physics and Information Engineering, Fuzhou University and Fujian Science & Technology Innovation Laboratory for Optoelectronic Information of China, Fuzhou, China. [3]Quantum Device Physics Laboratory, Department of Microtechnology and Nanoscience, Chalmers University of Technology, Gothenburg, Sweden. [4]School of Physics and Electronic Information, Weifang University, Weifang, China. [5]Institute of Microelectronics, Chinese Academy of Sciences, Beijing, China. ✉e-mail: jie.sun@fzu.edu.cn; guoweiling@bjut.edu.cn

of few-layer graphene is fabricated. In this scheme, the Ni auxiliary layer is cleverly used as a mask for dry etching and as a catalyst for graphene growth, which is removed after graphene growth to achieve patterning preparation of transfer-free graphene. On this basis, a SiO_2 isolation layer is introduced, which avoids the fusion of the substrate and the Ni auxiliary layer at high temperatures. This key makes the technique suitable not only for insulators but also for semiconductors and metals, ensuring the transfer-free preparation of graphene on diverse materials such as GaN and Au. In this paper, the high quality and high uniformity of the prepared 2-inch wafer-scale graphene were confirmed by a variety of characterization methods, and the improvement effect of graphene TEs on LED performance was deeply analyzed. In addition, through detailed comparison with other advanced graphene preparation techniques, this method shows certain advantages, providing a new solution for the scalable application of graphene.

Results

Figure 1 is a schematic diagram of the process flow of a 2-inch wafer-scale LED chip with transfer-free patterned graphene as TEs. Eight of the images show the status of the sample at different stages, and the corresponding process operations are indicated between the two adjacent images.

Figure 2 is a physical image of the 2-inch sample at different process stages, and the inset is a 50x optical image. Figure 2a–h corresponds to the eight sample structure schematics in Fig. 1. Since the 4-inch epitaxial wafer cannot be divided into circles, the sample in this paper is a square with a side length of about 3.6 cm, which is approximately the inscribed square of a 2-inch circle (Fig. 2a). First, photolithography is performed following the pattern of the LED mesas, SiO_2 isolation layer and Ni auxiliary layer are deposited, and then lift-off (Fig. 2b). Among them, Ni is not only a mask for etching LED mesas, but also a catalyst for graphene growth. The SiO_2 isolates the substrate from Ni, preventing the two from fusing at high temperatures while growing graphene, thus protecting both the integrity of the substrate and the catalytic properties of Ni. Relevant experiments were designed to verify the protective effect of the isolation layer (Figs. S1–S3). The LED mesas are obtained by dry etching with Ni as a mask (Fig. 2c). As can be seen from the inset, the Ni surface is slightly yellowed after etching, possibly due to oxidation of the Ni mask by etching gas or plasma bombardment. Therefore, the sample is treated under H_2 before growing graphene to reduce this effect. In Fig. 2d, graphene is grown on the sample by plasma enhanced chemical vapor deposition (PECVD). It can be seen that the size of the heating stage is only 2 inches round, which is why the sample size in this paper is limited to 2 inches. Figure 2e shows that poly(methylmethacrylate) (PMMA) is spin-coated onto the sample surface after graphene growth. Then Ni and SiO_2 are removed by penetration etching (Fig. 2f). The so-called penetration etching is the etching solution passing through the PMMA and graphene films, causing the Ni and SiO_2 to be slowly etched away. Although the Ni film in direct contact with the graphene is etched away, the graphene does not float away, but is fixed above the mesa by PMMA in close contact with n-GaN, and falls on the surface of p-GaN after penetration etching. Even if there is PMMA on the surface of the sample, it can be seen in the inset that the silvery-gray Ni on the LED mesas is no longer present, and the entire sample surface is dark blue under the microscope. The PMMA film is removed so that the graphene on the p-GaN is exposed (Fig. 2g). Finally, the metal electrodes of the LEDs are prepared (Fig. 2h).

In addition, the fabricated LED devices were characterized by Energy Dispersive Spectrometer to observe the elemental composition of the surface (Table 1). The Ti and Au elements are derived from the metal electrodes, and the In element is derived from the InGaN layer in the epitaxial wafer. There are no Si and Ni elements on the surface of the sample, which means that SiO_2 isolation layer and Ni auxiliary layer have been essentially etched away, verifying the effectiveness of penetration etching.

In order to observe the specific state of the graphene prepared on the sample, the scanning electron microscope (SEM) characterization results are shown in Fig. 3. Figure 3a shows a 120x SEM image of the LED device (left) and a 5000x SEM image of graphene on a mesa (right). In addition, for ease of observation, the area characterized in the image on the right is a deliberately selected area where graphene is broken. It can be seen that the mesa is almost completely covered with graphene, with only a very small bright white area without graphene (the validation of the Raman spectra is shown in Fig. S4). Graphene exhibits an overall uniform black and gray alternation pattern, which may be caused by small differences in the number of graphene layers in different positions. Since the prepared graphene is few layers (about 3–10), there is not much difference in the Raman spectra of graphene in the black and gray areas (Fig. S4). Therefore, the prepared graphene can be considered to cover the entire mesa evenly.

To investigate the quality and uniformity of graphene on the entire 2-inch sample, graphene at 30 locations (dark blue dots in Fig. 3b) was uniformly and randomly selected to be characterized by SEM (Fig. 3b). It can be seen that the flake pattern of graphene near the edges is smaller and denser across the sample, which may be due to the difference in the actual temperature of the edge and center of the sample during graphene growth. Because of the inevitable lattice mismatch in the GaN epitaxial wafer with sapphire as the substrate, the stress generated by it causes the entire 2-inch

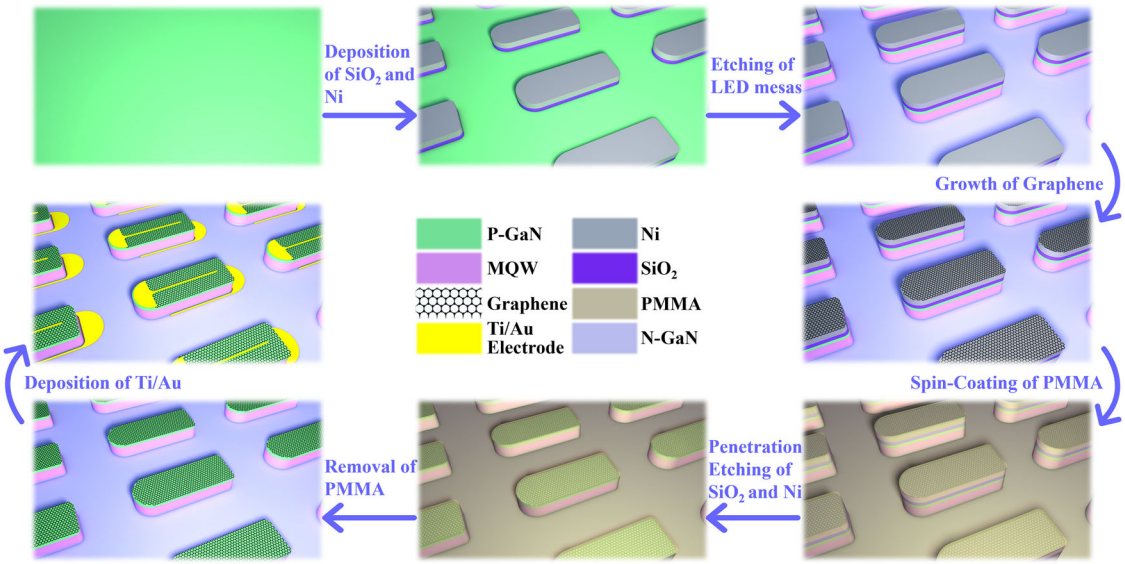

Fig. 1 | Schematic diagram of the process flow of a 2-inch wafer-scale LED chip with transfer-free patterned graphene as TEs. *MQW* multiple quantum well.

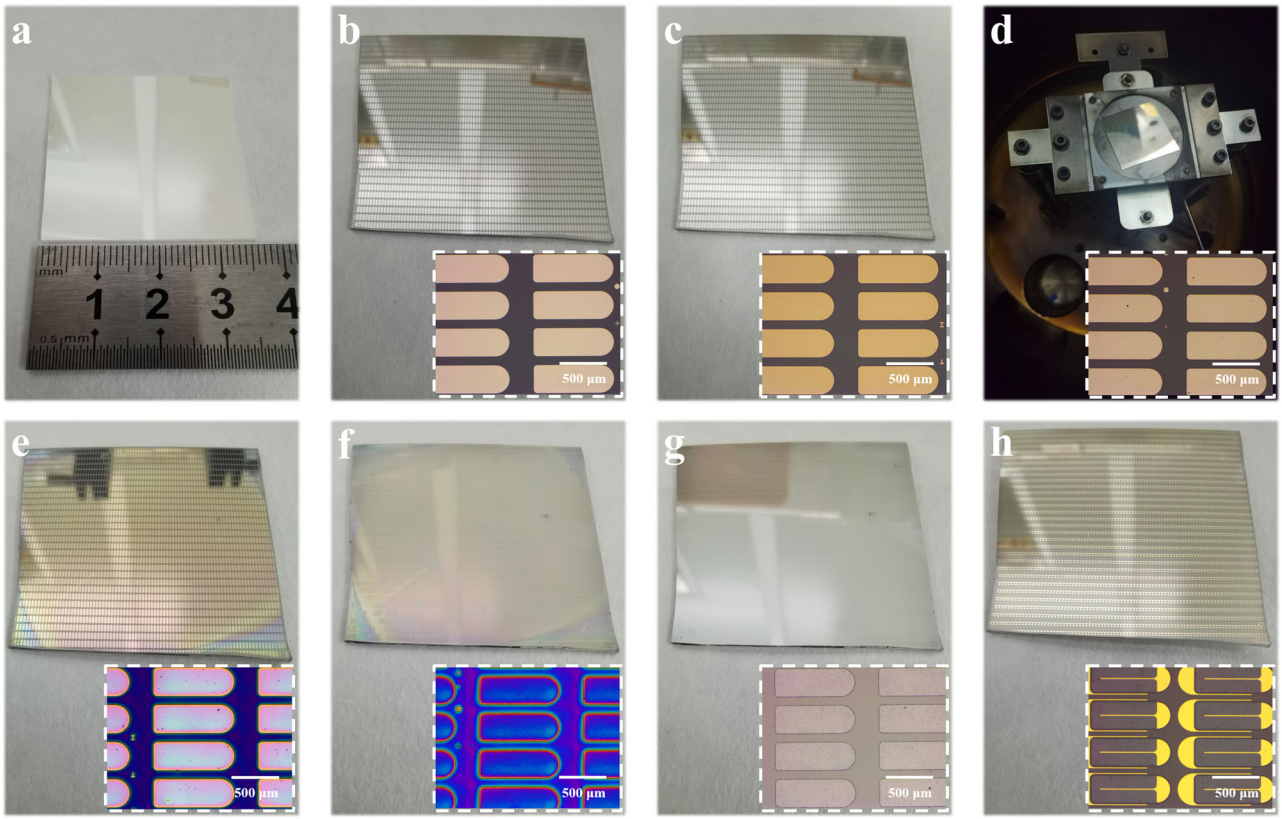

Fig. 2 | Physical images and 50x optical images of the sample at different process stages. a The initial square sample had a side length of about 3.6 cm. The long and blurred stripes are mirror images of the patterns from the ceiling. **b** SiO_2 and Ni in the shape of the LED mesas were deposited. The inset is a 50x optical image, the same below. **c** The 1.3 μm deep LED mesas were obtained by the inductively coupled plasma reactive ion etching (ICP-RIE). **d** The sample after graphene growth on the heating stage in PECVD. **e** PMMA was spin-coated and dried. **f** Ni and SiO_2 were removed by penetration etching. **g** PMMA was removed. **h** Ti/Au electrodes were prepared.

Table 1 | The element content of the surface layer of the fabricated LEDs

	C	N	Ga	Au	Ti	In	Ni	Si
Weight%	9.83	11.58	64.16	13.21	0.37	0.85	–	–
Atom%	30.91	31.23	34.76	2.53	0.29	0.28	–	–

sample to be not absolutely "horizontal". It may result in different regions of the sample and the heating stage in different degrees of contact in the graphene growth, and small temperature differences have an impact on the morphology of the graphene. Fortunately, the differences in graphene at different locations are so small that they need not be considered. Therefore, it can be inferred that the graphene prepared by this method has good consistency on the scale of 2-inch wafer. In the future, the uneven heating caused by stress can be alleviated through substrate optimization engineering, so as to further improve the uniformity of graphene.

The prepared transfer-free graphene was characterized in more ways to further understand its properties, and the characterization results are shown in Fig. 4. Figure 4a is a high-resolution transmission electron microscope (HRTEM) image of graphene, and the inset is an image of graphene being transferred to a copper grid. Although the graphene in the LED devices in this paper does not need to be transferred, the transfer-free graphene prepared on GaN cannot be directly characterized by HRTEM, so it has to be transferred to the surface of the copper grid. The edge of graphene is marked in a red box, from which it can be inferred that the number of layers of the graphene is about 5–6 layers. For serious consideration, the number of layers of the overall graphene may fluctuate in a wider range (about 2–10). Figure 4b is a selected area electron diffraction (SAED) image of graphene. Several diffraction spots can be seen connected into bright short lines, which may also indicate that the prepared graphene is few-layered.

Figure 4c shows the transmission spectrum of the prepared graphene at 300–750 nm, and the electroluminescence spectrum of the LED is also labeled in the figure (blue area). The transmittance of graphene at the peak wavelength (455 nm) of the LED was observed to be approximately 91.6%. In addition, the sheet resistance of graphene was measured by the circular transmission line method (CTLM)[35], and a schematic diagram of the sample preparation process is shown in Fig. S5. The inset in Fig. 4d shows the optical image of the measurement. In the measurement, a pair of probes is in contact with metal electrodes inside and outside the "graphene ring". The inner diameter of these six rings is 76 μm, and the outer diameters are 79, 84, 92, 100, 108, and 120 μm, respectively. Figure 4d shows the current-voltage characteristic curves corresponding to the six rings, from which the linear relationship between total resistance R_T and $\ln\left(\frac{r_n}{r_0}\right)$ in Fig. 4e is fitted. The sheet resistance of graphene is calculated to be 423.9 Ω sq^{-1}, and the contact resistance between graphene and metal electrodes is calculated to be 5.103×10^{-4} Ω cm^2.

In order to better observe the state of graphene at different experimental stages and explore the effects of penetration etching and electrode preparation on the graphene, graphene was characterized by Raman when it was in three different stages (Fig. 4f). There are three common Raman characteristic peaks of graphene: D peak at 1350 cm^{-1}, G peak at 1580 cm^{-1}, and 2D peak at 2700 cm^{-1}. The ratio of the 2D peak to the G peak is usually related to the number of layers of graphene, and the larger the ratio, the fewer layers of graphene. The D peak is generally associated with the defects of graphene, and the higher its strength, the more defects in graphene[36]. The Fig. 4f shows the Raman spectra of as-grown graphene on the Ni surface, of

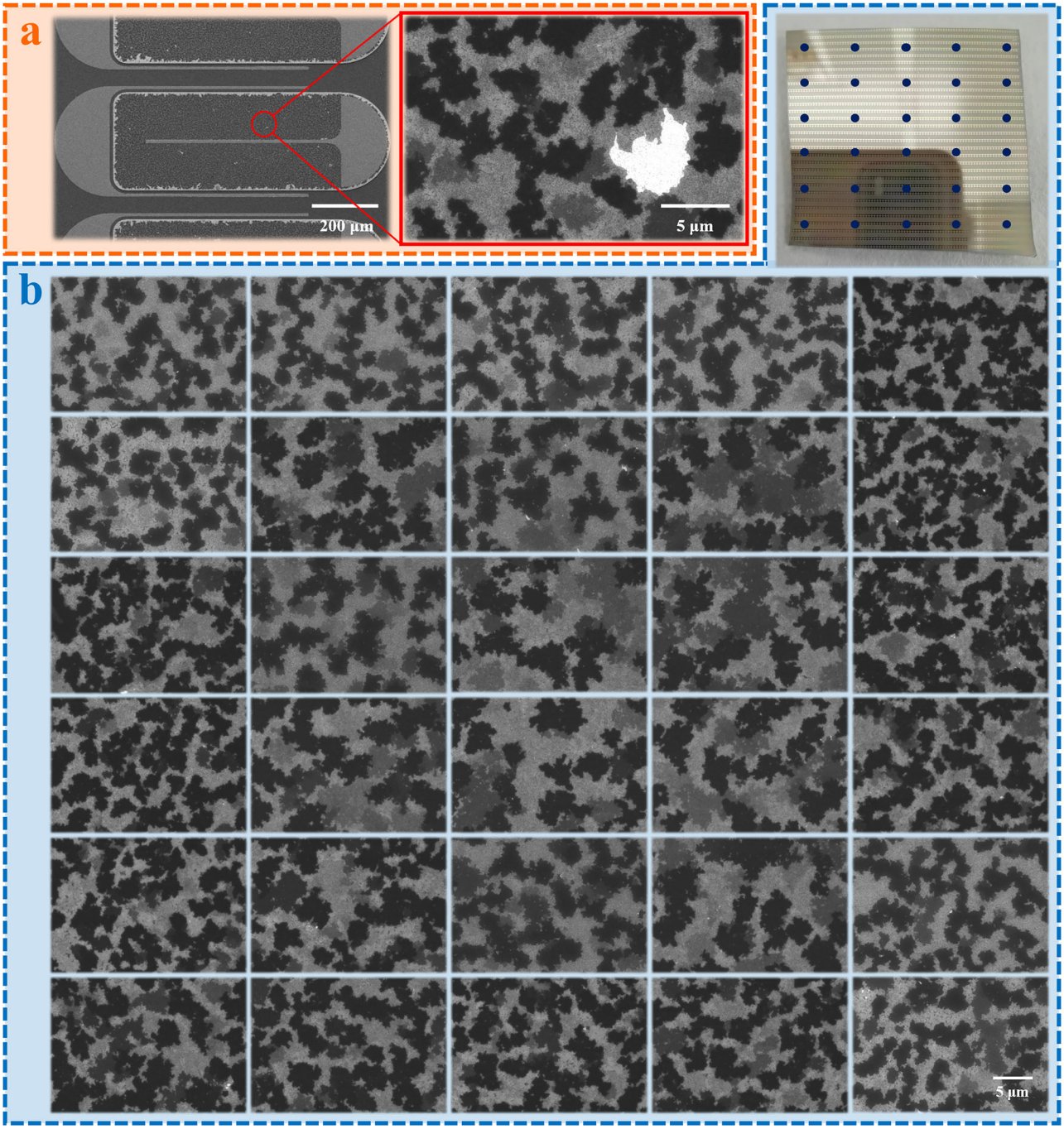

Fig. 3 | SEM characterizations of graphene and LED devices. a SEM images of graphene and LED at two magnifications. **b** SEM images of graphene in different areas across the entire 2-inch sample. The inset is an optical image of the 2-inch sample, and the shadow in the lower left corner is the reflected image of the camera. 30 points (blue dots in this image) were randomly selected uniformly on the entire sample to observe the overall uniformity and quality of the graphene.

the graphene falling on the p-GaN surface after penetration etching, and of the graphene on the final LED device after electrode preparation. In addition, GaN has messy Raman peaks at 100–1500 cm^{-1}, which will superimpose with the Raman peaks of graphene on the surface of GaN and cause interference, so the Raman spectrum of GaN is also shown in Fig. 4f for reference. It can be seen that there is no significant difference in the Raman spectra of graphene at different stages, which indicates that the process after graphene preparation has almost no effect on the quality of graphene. In addition to this, the intensity of the D peak of graphene in these Raman spectra is very small, and the intensity of the 2D peak is about half that of the G peak. It indicates that the prepared graphene has few defects and good quality, and once again confirms that it is few-layered.

One of the outstanding advantages of this paper is the 2-inch wafer-scale preparation of high-quality graphene, so in addition to the SEM characterizations described above, the sample is also characterized by Raman mapping to fully and accurately observe the overall uniformity and quality of the graphene. In this part, two Raman mapping characterization methods are employed. One is a dense sampling (30×30 points) of graphene in a randomly selected small area (40×40 μm^2), as shown in Fig. 5a. It can reflect the uniformity of graphene in a small area on the 2-inch sample, which is referred to below as local Raman mapping (LRM). The other is the scattered sampling of 9×9 measured points evenly and randomly selected on the 2-inch sample, as shown in Fig. 5d. It reflects the uniformity trend of the wafer-scale graphene, which is referred to below as overall Raman

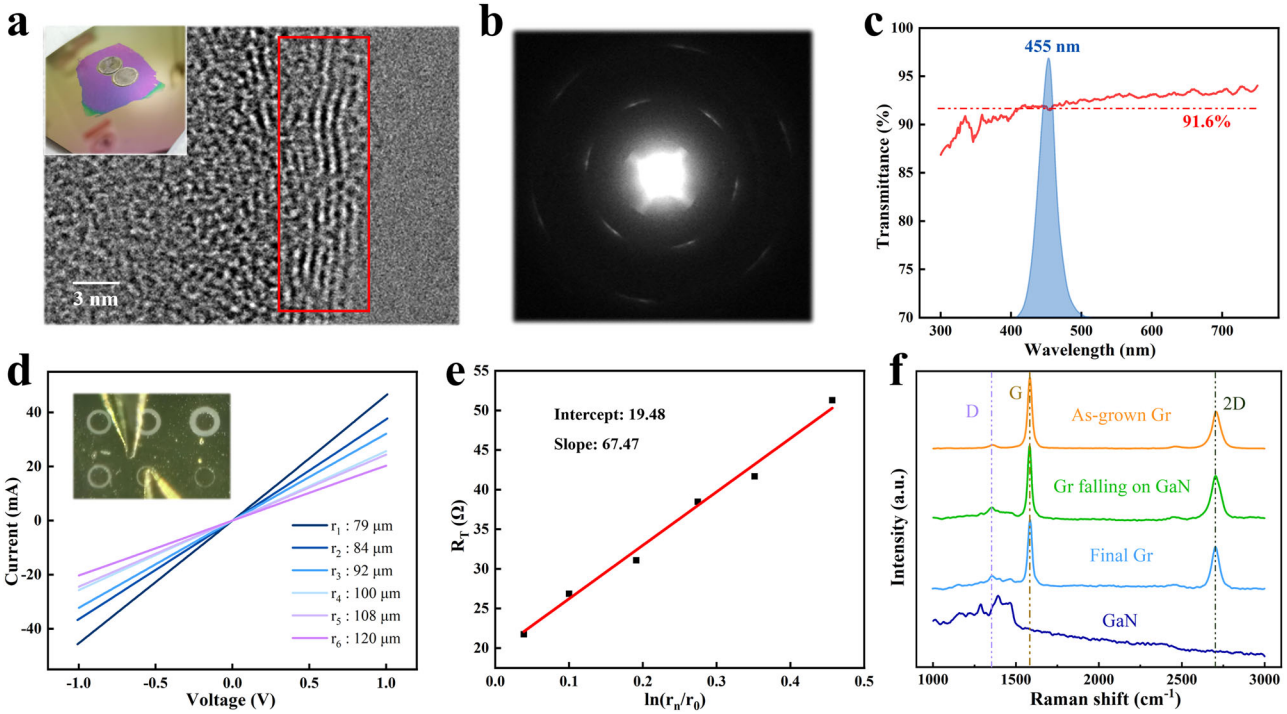

Fig. 4 | Performance characterizations of the prepared transfer-free graphene. **a** HRTEM image of graphene. Since the transfer-free graphene prepared on GaN cannot be characterized by HRTEM, the graphene is transferred to the surface of the copper grid (shown in the inset). Inside the red box is the edge of graphene. **b** SAED image of graphene. **c** The transmission spectrum of the prepared graphene in the range of 300–750 nm, and the blue area represents the electroluminescence spectrum of the fabricated LEDs in this paper. **d** The sheet resistance of graphene is measured according to the CTLM. The current-voltage characteristic curves of the rings with different outer diameters are shown. The inset is an optical image of the measurement. **e** The linear relationship between R_T and $\ln\left(\frac{r_n}{r_0}\right)$ fitted from the data in (**d**). **f** Raman spectra of graphene at different process stages. "As-grown Gr" represents graphene that has just grown from the surface of Ni; "Gr falling on GaN" represents the graphene that falls on the surface of p-GaN after penetration etching; "final graphene" represents the graphene after the electrode prepared; "GaN" represents the Raman spectrum of GaN.

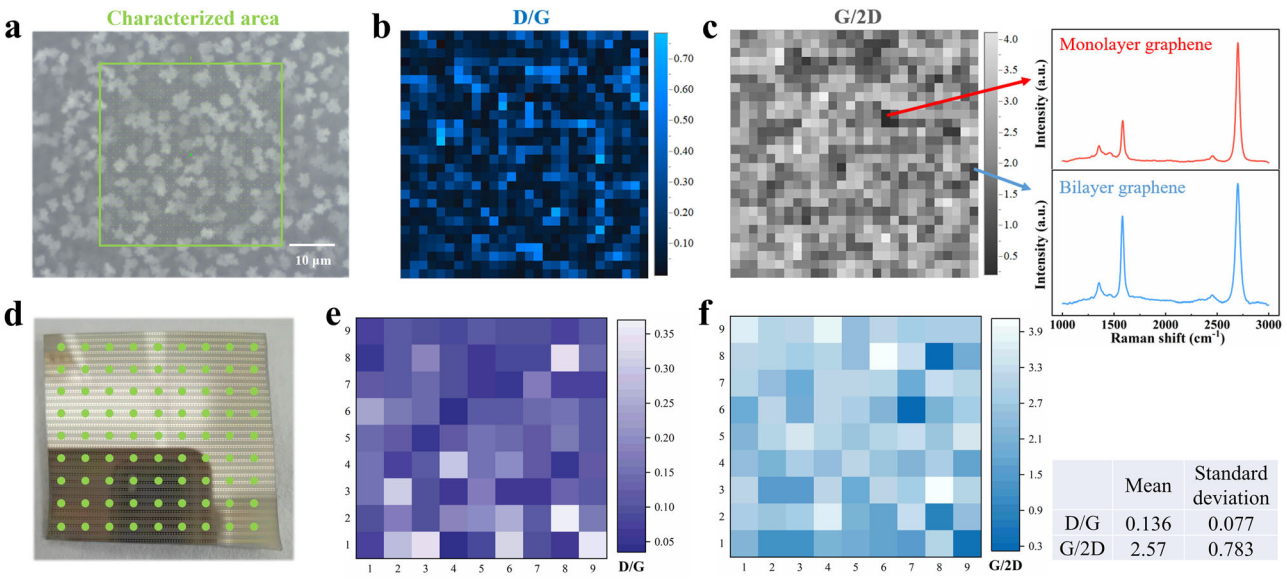

Fig. 5 | Raman mapping characterizations of graphene TEs on LEDs. **a**–**c** show the LRM characterization results and (**d**, **e**) show the ORM characterization results. The overall quality and uniformity of graphene on the 2-inch sample can be inferred through the comprehensive analysis of the two. **a** The characterized area of LRM (in the green box) which corresponds to the graphene on a mesa. **b** D/G image of LRM. **c** G/2D image of LRM. **d** The characterized area of ORM, and the shadow in the lower left corner is the reflected image of the camera. The measured points are approximated as the green dots in this image. **e** D/G image of ORM. **f** G/2D image of ORM.

mapping (ORM). By combining the characterization results of the two, more accurate uniformity and quality of graphene at the 2-inch scale can be inferred.

Figure 5a–c is the LRM characterization results, and Fig. 5d–f is the ORM characterization results. Each set of images shows the measured area, the ratio of peak D to peak G (D/G), and the ratio of peak G to peak 2D (G/2D). Because the graphene prepared is mainly of few layers, only individual regions are mono- or bi-layer, for more intuitive observation, G/2D is shown instead of the common 2D/G. First, the G/2D of the two characterization methods was compared. It can be seen that there is a fairly high degree of consistency between the results of LRM and ORM, with G/2D ranging from 0.3 to 4. The high uniformity of the prepared graphene was further demonstrated. Among them, most of the G/2D data are between 2 and 4, and only a small number of G/2D data are below 1, which indicates that the prepared graphene is dominated by few-layer graphene and very few areas are mono- or bi-layer graphene (shown in Fig. 5c). Then, the D/G of the two characterization methods were compared. It is worth noting that the D/G of LRM is between 0.05 and 0.75, while the D/G of ORM is between 0.05 and 0.35. As mentioned earlier, the GaN Raman peaks at 1000–1500 cm^{-1} are superimposed on the D peak of graphene, interfering with the observation. Since the LRM image is automatically generated in real time by the Raman spectrometer during the measurement, it cannot eliminate the interference of the GaN Raman peaks, so the measured intensity of D peak is greater than the actual value. While the ORM image is artificially drawn based on the Raman spectra after deducting the influence of GaN, which is more realistic. Therefore, the results of Fig. 5b, e are actually essentially consistent, both between 0.05 and 0.35. Through statistical analysis of ORM data, the properties of graphene on the 2-inch sample were obtained: The mean value of D/G is 0.136, and the standard deviation is 0.077; The mean value of G/2D is 2.57, and the standard deviation is 0.783. The results show that the prepared graphene is a few-layer graphene with few defects, and the uniformity is not bad. This verifies the effectiveness of the proposed preparation technique for transfer-free patterned graphene.

To investigate the role of graphene as a TE in LEDs, three different LEDs were fabricated (graphene-free, graphene only under metal electrodes, and complete graphene TE). Among them, the LED with graphene only under electrodes is obtained by the LED with complete graphene being treated with oxygen plasma so that the graphene exposed on p-GaN is removed, in which graphene only exists between the metal electrodes and p-GaN. Figure 6a shows the voltage and internal resistance of a graphene-free LED as a function of current, and the inset shows its luminescence image at 1 mA (~6.5 V). Figure 6b shows the electrical characteristic curves of the other two LEDs and their luminescence images at 20 mA (~3–4 V). It can be seen that the graphene-free LED has a particularly low current (only 1.41 mA at 7 V) due to the failure to form a good ohmic contact between the metal electrode and p-GaN. Compared with it, the two LEDs with graphene have far better current-voltage characteristics, which indicates that graphene as an intermediate layer greatly improves the ohmic contact between the electrode and p-GaN, greatly improving the electrical performance of the LEDs. Among them, the LED with complete graphene TE has relatively lower turn-on voltage and internal resistance, which may be due to the current spreading effect of graphene on p-GaN. As can be seen from the luminescent images: the graphene-free LED only emits a faint blue light from the part of the mesa under the electrode; the LED with graphene only

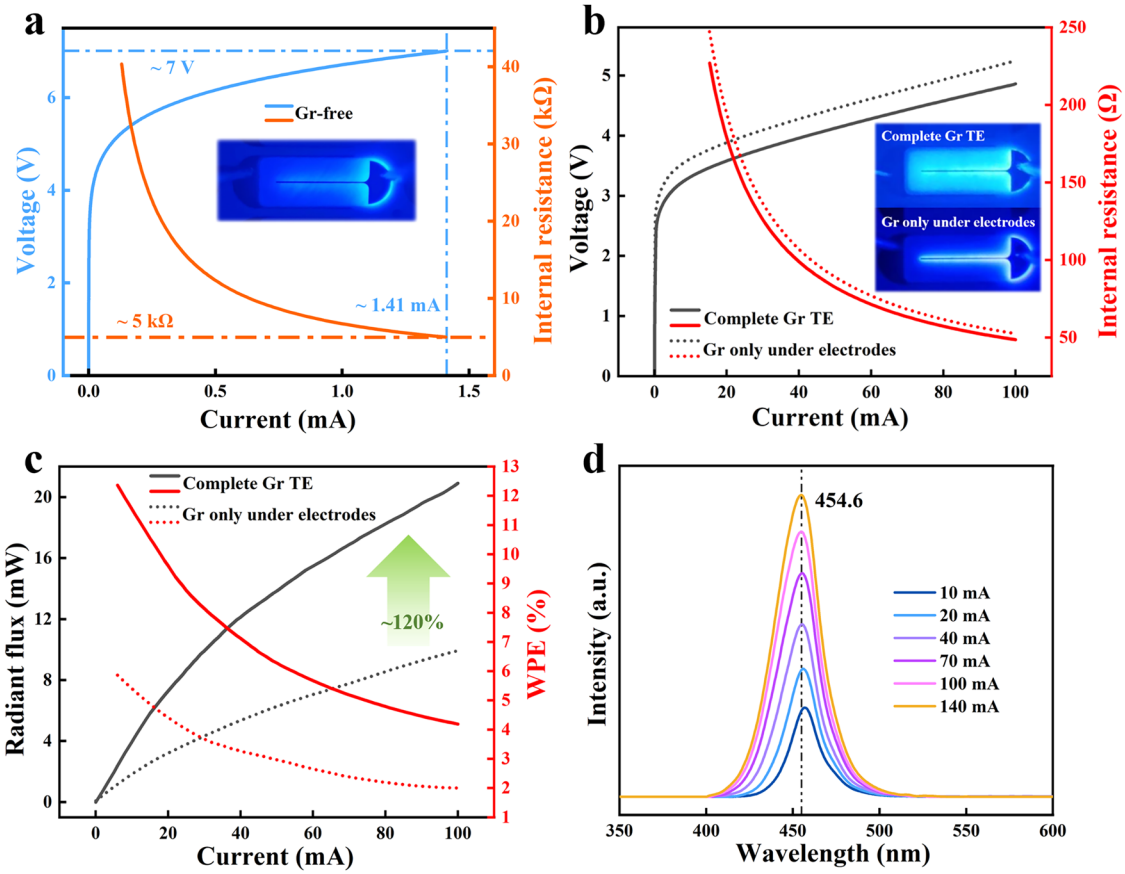

Fig. 6 | Electrical and optical properties of different LED devices. a Voltage and internal resistance curves of the graphene-free LED as a function of current, and inset is a luminous image at 1 mA. **b** Voltage and internal resistance curves of the two LEDs with graphene TEs as a function of current. The insets are their luminous images at 20 mA. **c** Curves of radiant flux and WPE variation with current of the two LEDs with graphene TEs. **d** Electroluminescence spectra of the LED with complete graphene TE at different currents. The peak wavelength is about 454.6 nm.

under electrode emits bright light from under the electrode; the LED with complete graphene TE emits a bright and uniform light from the entire mesa. This further directly confirms the role of graphene in improving electrode contact and current spreading.

Figure 6c shows the radiant flux and wall plug efficiency (WPE) curves for the two LEDs as a function of current. Graphene-free LEDs are not optically characterized because too little light is emitted. It can be seen that although the electrical properties of the LED with complete graphene TE are only slightly better than that of the LED with graphene only under electrodes, the optical properties are about 220% of its, which is attributed to the current spreading of graphene to expand the effective luminous area. In order to better demonstrate the performance of the LED with complete graphene TE, the electroluminescence spectra at different currents are shown in Fig. 6d. With the increase of current, the electroluminescence spectrum is slightly blue-shifted, and then the peak wavelength gradually stabilizes to 454.6 nm. This is because when the injection current increases, the charge screening weakens the polarized electric field in MQW, which in turn weakens the quantum-confined Stark effect. In addition, the band-filling effect also causes the electroluminescence spectrum of the LED to be blue-shifted as the current increases.

The fabricated 2-inch LED chip with complete graphene TE was also characterized as a whole to observe the uniformity of the electrical and optical properties of LEDs. The characterization method is similar to the ORM described above; that is, dozens of devices are uniformly selected randomly on the entire sample for measurement, and then the relevant mapping images are drawn based on the measurement results. Voltage mapping images of 7 × 7 LEDs at 20 mA (Fig. 7a) and 100 mA (Fig. 7b), as well as radiant flux mapping images at 20 mA (Fig. 7c) and 100 mA (Fig. 7d) are shown. It can be seen that the electrical and optical properties of the LEDs at different positions change by a small amplitude, indicating that the LEDs across the 2-inch wafer have good consistency in performance. In order to more visually demonstrate the uniformity and yield of the LEDs, 9 × 9 LEDs were uniformly selected at random, and their luminous images at 20 mA were shown in Fig. 7e. The images show that even the LEDs at the

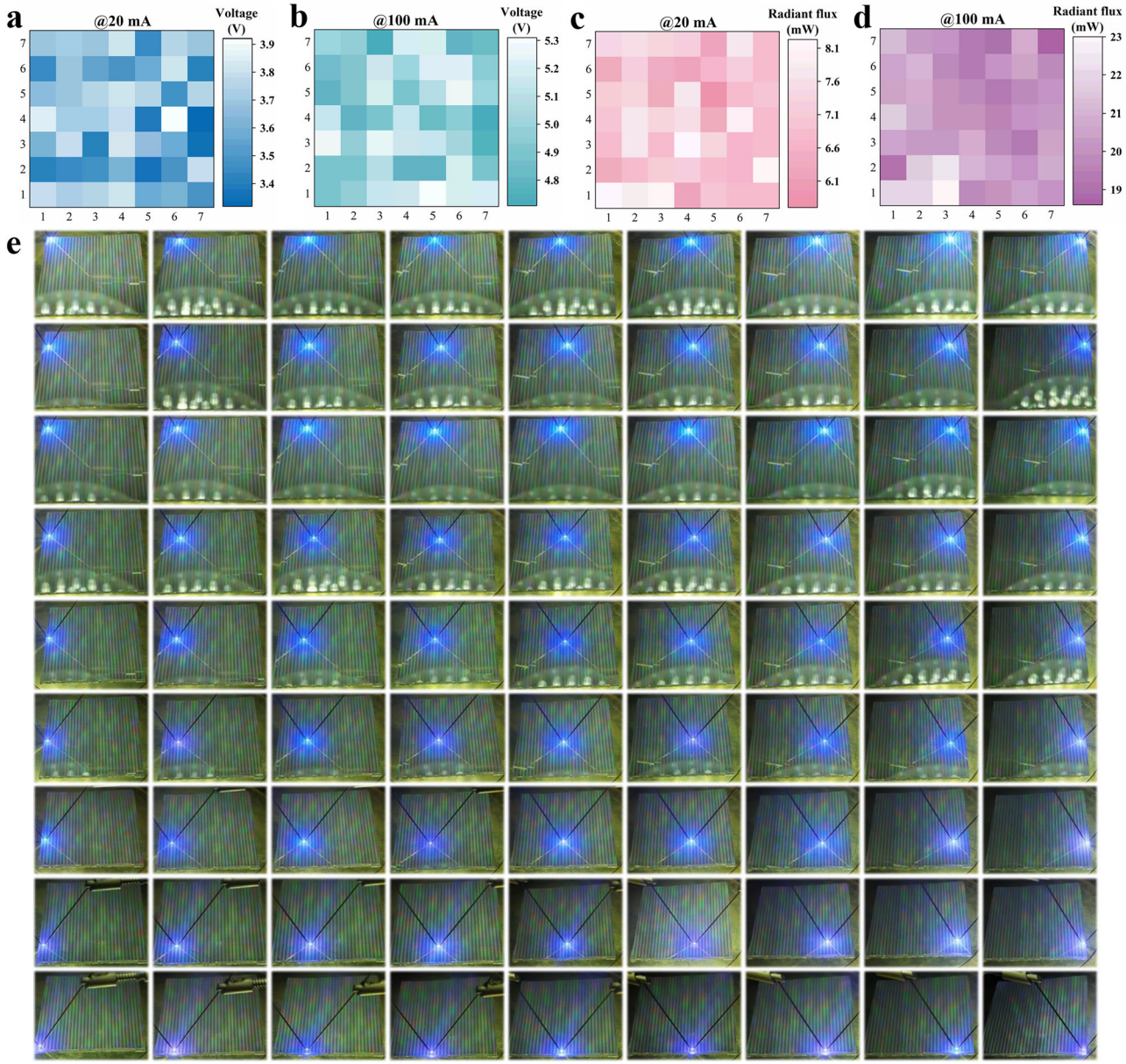

Fig. 7 | Characterizations of the overall performance of the LEDs on the 2-inch sample. 7 × 7 LEDs in (**a**–**d**) and 9 × 9 LEDs in (**e**) are evenly randomly selected. **a** Voltage mapping image of LEDs at 20 mA. **b** Voltage mapping image of LEDs at 100 mA. **c** Radiant flux mapping image of LEDs at 20 mA. **d** Radiant flux mapping image of LEDs at 100 mA. **e** Luminous images of LEDs at different positions at 20 mA.

Table 2 | Comparison of several graphene preparation studies in terms of technical characteristics, process conditions, and graphene properties

Wafer scale (inch)	Transfer process	Applicable substrates	Patterning process	Temperature (°C)	Growth Time (min)	Number of layers	Sheet resistance (kΩ/□)	Ref.
6	Require	–	Require	1000	20	1	–	30
–	Require	–	Require	1005	20	1	0.314	16
–	Free	Glass	Require	600	2	10–16	0.97–1.6	22
2	Free	SiO_2	Require	300	40	1	0.09–0.12	29
2	Free	SiC	Require	1550	5-8	2–3	0.72	26
4	Free	Quartz and other insulators	Require	1050–1080	60-300	1–2	1.8–2.2	31
2	Free	SiO_2 and other insulators	Require	900	5	1–3	2	23
4	Free	SiO_2 and other insulators	Require	1060–1120	90	1	1.409	32
4	Free	Parylene	Free	935	20–60	7–17	0.23–0.57	28
–	Free	SiO_2 and other insulators	Free	950	0.5	1	20-50	25
–	Free	SiO_2 and other insulators	Free	1000	7–20	2	2	24
2	Free	Insulators, metals and semiconductors	Free	650	10	3–10	0.424	This work

edges or corners of the sample have the same luminous performance as other LEDs. In addition, each LED selected can emit light normally, even if this does not indicate that all the LED devices are qualified, but it is enough to prove that the fabricated LEDs have a very high yield. This also means that graphene as TEs is generally effective on the whole sample, which once again proves that the 2-inch wafer-scale graphene prepared by this method has high uniformity and quality.

Discussion

Table 2 compares the technical advantages, process conditions and graphene characteristics of the twelve graphene preparation methods. First of all, the preparation scale of graphene is compared, and the wafer-scale of more than two inches is marked. Then, it is indicated whether the graphene prepared by each technique requires a transfer process or a patterning process when it is oriented to the application. For the transfer-free preparation techniques, the substrate materials applicable to it are also listed. In terms of process conditions, the growth temperature and time were compared, and in terms of graphene characteristics, the number of graphene layers and sheet resistance were compared. It can be seen that our technique has a relatively low growth temperature and time, which is more substrate-friendly and simplifies the process, and the prepared few-layer graphene exhibits a relatively low sheet resistance. Most importantly, this technique enables 2-inch wafer-scale, transfer-free and patterned graphene preparation, and is suitable for a wider variety of substrates than other techniques.

In conclusion, in this paper, a patterning preparation technique of 2-inch wafer-scale transfer-free graphene is proposed, and a GaN-based LED chip with graphene TEs are fabricated accordingly. The high uniformity and quality of graphene at the 2-inch scale are demonstrated by the overall characterizations of the sample. From the electrical and optical measurement results of the LEDs, it can be seen that graphene as a transparent electrode shows excellent effect on improving electrode contact and current spreading. The core of the technique is mainly in three aspects. First of all, the penetration etching process is the basic principle and important method for the preparation of transfer-free graphene. Secondly, the Ni auxiliary layer plays the role of etching mask and graphene growth catalyst, realizing the patterning growth of graphene. Finally, the SiO_2 isolation layer provides great protection for the substrate and Ni, making the technique suitable for most electronic materials such as semiconductors (e.g., GaN, SiC), metals (e.g., Au) and insulators (e.g., SiO_2, quartz). In addition, the current scale of the technique is only a 2-inch wafer due to the limitation of the sample stage size of the PECVD growing graphene, so it can be developed to a larger scale in the future by optimizing the process equipment. In short, the scheme proposed in this paper is concise and efficient, integrates the advantages of the current graphene preparation techniques, and provides a new solution for the industrial integration of graphene and electronic devices.

Methods

First, photolithography is performed following the pattern of the LED mesas, SiO_2 and Ni are deposited, and then lift-off. Here, the two materials are patterned in a single step, which not only simplifies the process but also ensures that SiO_2 is completely isolated from Ni and GaN. It is worth noting that due to the compressive and tensile stress in the film, the thickness of Ni should not be too thick (200 nm in this work) and the thickness of SiO_2 should not be too thin (170 nm in this work) to avoid Ni/SiO_2 film falling off the GaN surface due to stress during the lift-off. With Ni as mask. The LED mesas of 300 × 700 μm^2 were obtained by ICP-RIE, and the etching depth is ~1.25 μm. After etching, the Ni layer remains about 160 nm. The sample is then treated for 10 min in an atmosphere of $CH_4/H_2/Ar$ (15/20/960 sccm) at 60 W plasma power, 650 °C and 6 mbar in a cold-walled PECVD. In this process, graphene grows on the surface of Ni under its catalytic action. Then PMMA was spin-coated on the sample surface (3000 r/min for 30 s) and baked at 150 °C on a heating stage for 10 min. After natural cooling, Ni and SiO_2 are etched away by penetration etching. Because the Ni is on the surface of the SiO_2, the sample is first soaked in etching solution A ($CuSO_4$: HCl: H_2O = 10 g: 50 ml: 50 ml) for 3 h to remove the Ni from the SiO_2. After the sample is removed from etching solution A, it is soaked in deionized water for 20 min. It is then soaked in etching solution B (HF: NH_4F: H_2O = 3 ml: 6 g: 60 ml) for 3 h to remove the SiO_2. After the etching is finished, the sample is soaked in deionized water again for 30 min, and then it is removed and naturally dried. In order to strengthen the contact between graphene and p-GaN, the sample is baked at 150 °C for 10 min. PMMA is subsequently removed by acetone and isopropanol, and the sample is cleaned in slow-flowing deionized water for 10 min. Finally, metal electrodes (15 nm Ti and 80 nm Au) are deposited on the sample.

Data availability

No datasets were generated or analysed during the current study.

Received: 28 February 2025; Accepted: 23 June 2025;
Published online: 24 July 2025

References

1. Novoselov, K. S. et al. Electric field effect in atomically thin carbon films. *Science* **306**, 666–670 (2004).

2. Nair, R. R. et al. Fine structure constant defines visual transparency of graphene. *Science* **320**, 1308 (2008).
3. Lee, C., Wei, X., Kysar, J. W. & Hone, J. Measurement of the elastic properties and intrinsic strength of monolayer graphene. *Science* **321**, 385–388 (2008).
4. Gao, N. & Fang, X. S. Synthesis and development of graphene −inorganic semiconductor nanocomposites. *Chem. Rev.* **115**, 8294–8343 (2015).
5. Nakamura, S., Mukai, T., Senoh, M. & Iwasa, N. Thermal annealing effects on p-type Mg-doped GaN films. *Jpn. J. Appl. Phys.* **31**, L139–L142 (1992).
6. Kang, D. Y. et al. Dopant-tunable ultrathin transparent conductive oxides for efficient energy conversion devices. *Nano Micro Lett.* **13**, 211 (2021).
7. Kim, B.-J. et al. Large-area transparent conductive few-layer graphene electrode in GaN-based ultra-violet light-emitting diodes. *Appl. Phys. Lett.* **99**, 143101 (2011).
8. Jiang, G. et al. An efficient flexible graphene-based light-emitting device. *Nanoscale Adv.* **1**, 4745–4754 (2019).
9. Miao, J. & Fan, T. Flexible and stretchable transparent conductive graphene-based electrodes for emerging wearable electronics. *Carbon* **202**, 495–527 (2023).
10. Kang, J. H. et al. Cu/graphene hybrid transparent conducting electrodes for organic photovoltaic devices. *Carbon* **171**, 341–349 (2021).
11. Park, I.-J., Kim, T. I. & Choi, S.-Y. Charge transfer dynamics of doped graphene electrodes for organic light-emitting diodes. *ACS Appl. Mater. Interfaces* **14**, 43907–43916 (2022).
12. Ma, L.-P. et al. Stably doped graphene transparent electrode with improved light-extraction for efficient flexible organic light-emitting diodes. *Nano Res.* **16**, 12788–12793 (2023).
13. Adetayo, A. E., Ahmed, T. N., Zakhidov, A. & Beall, G. W. Improvements of organic light-emitting diodes using graphene as an emerging and efficient transparent conducting electrode material. *Adv. Opt. Mater.* **9**, 2002102 (2021).
14. Pekdemir, S., Onses, M. S. & Hancer, M. Low temperature growth of graphene using inductively-coupled plasma chemical vapor deposition. *Surf. Coat. Technol.* **309**, 814–819 (2017).
15. Li, X., Cai, W., Colombo, L. & Ruoff, R. S. Evolution of graphene growth on Ni and Cu by carbon isotope labeling. *Nano Lett.* **9**, 4268–4272 (2009).
16. Roh, J. S. et al. Macroscopic properties of single-crystalline and polycrystalline graphene on soft substrate for transparent electrode applications. *Carbon* **178**, 181–189 (2021).
17. Han, X. et al. Twist-angle controllable transfer of 2D materials via water vapor intercalation. *Adv. Mater.* **37**, 2417052 (2025).
18. Chen, S. et al. Tunable adhesion for all-dry transfer of 2D materials enabled by the freezing of transfer medium. *Adv. Mater.* **36**, 2308950 (2024).
19. Hu, Z. et al. Rapid and scalable transfer of large-area graphene wafers. *Adv. Mater.* **35**, 2300621 (2023).
20. Liu, Q., Gong, Y., Wang, T., Chan, W.-L. & Wu, J. Metal-catalyst-free and controllable growth of high-quality monolayer and AB-stacked bilayer graphene on silicon dioxide. *Carbon* **96**, 203–211 (2016).
21. Khan, A. et al. Direct CVD growth of graphene on technologically important dielectric and semiconducting substrates. *Adv. Sci.* **5**, 1800050 (2018).
22. Kamel, M. S. A., Stoppiello, C. T. & Jacob, M. V. Single-step, catalyst-free, and green synthesis of graphene transparent electrode for organic photovoltaics. *Carbon* **202**, 150–158 (2023).
23. Su, C.-Y. et al. Direct formation of wafer scale graphene thin layers on insulating substrates by chemical vapor deposition. *Nano Lett.* **11**, 3612–3616 (2011).
24. Peng, Z., Yan, Z., Sun, Z. & Tour, J. M. Direct growth of bilayer graphene on SiO_2 substrates by carbon diffusion through nickel. *ACS Nano* **5**, 8241–8247 (2011).
25. Kato, T. & Hatakeyama, R. Direct growth of doping-density controlled hexagonal graphene on SiO_2 substrate by rapid-heating plasma CVD. *ACS Nano* **6**, 8508–8515 (2012).
26. Jia, Y., Guo, L., Lin, J., Chen, L. & Chen, X. Wafer-scale graphene on 2 inch SiC with uniform structural and electrical characteristics. *Chin. Sci. Bull.* **57**, 3022–3025 (2012).
27. Dong, Y. et al. In situ growth of CVD graphene directly on dielectric surface toward application. *ACS Appl. Electron. Mater.* **2**, 238–246 (2020).
28. Babaroud, N. B. et al. Multilayer CVD graphene electrodes using a transfer-free process for the next generation of optically transparent and MRI-compatible neural interfaces. *Microsyst. Nanoeng.* **8**, 107 (2022).
29. Qian, F. et al. Transfer-free CVD growth of high-quality wafer-scale graphene at 300 °C for device mass fabrication. *ACS Appl. Mater. Interfaces* **14**, 53174–53182 (2022).
30. Kang, H. et al. Epitaxial growth of wafer scale antioxidant single-crystal graphene on twinned Pt(111). *Carbon* **181**, 225–233 (2021).
31. Jiang, B. et al. Batch synthesis of transfer-free graphene with wafer-scale uniformity. *Nano Res.* **13**, 1564–1570 (2020).
32. Ci, H. et al. Transfer-free quasi-suspended graphene grown on a Si wafer. *Adv. Mater.* **34**, 2206389 (2022).
33. Li, J. et al. Wafer-scale single-crystal monolayer graphene grown on sapphire substrate. *Nat. Mater.* **21**, 740–747 (2022).
34. Li, P. et al. Wafer-scale growth of single-crystal graphene on vicinal Ge(001) substrate. *Nano Today* **34**, 100908 (2020).
35. Wang, L. et al. Interface and transport properties of GaN/graphene junction in GaN-based LEDs. *J. Phys. D Appl. Phys.* **45**, 505102 (2012).
36. Ferrari, A. C. et al. Raman spectrum of graphene and graphene layers. *Phys. Rev. Lett.* **97**, 187401 (2006).

Acknowledgements

We thank the support from National Key Research and Development Program of China (2023YFB3608703 and 2023YFB3608700), National Natural Science Foundation of China (12474066), and Fujian Science & Technology Innovation Laboratory for Optoelectronic Information of China (2021ZZ122 and 2020ZZ110).

Author contributions

P.T. and J.S. designed the project. P.T. performed the experiments and wrote the original manuscript. Z.D. and A.F. assisted with experiments. J.L., R.W., G.P. and M.X. performed the measurements. W.G. analyzed the data. J.S. and W.G. revised the manuscript.

Funding

Open access funding provided by Chalmers University of Technology.

Competing interests

The authors declare no competing interests.

Additional information

Supplementary information The online version contains supplementary material available at https://doi.org/10.1038/s41699-025-00583-z.

Correspondence and requests for materials should be addressed to Jie Sun or Weiling Guo.